

# Nanofabrication and diffractive optics for high-resolution x-ray applications

Erik H. Anderson,<sup>a)</sup> Deirdre L. Olynick, Bruce Harteneck, Eugene Veklerov, Gregory Denbeaux, Weilun Chao, Angelic Lucero, Lewis Johnson, and David Attwood  
*E. O. Lawrence Berkeley National Laboratory, Mail Stop 2-400, 1 Cyclotron Road, Berkeley, California 94720*

(Received 15 June 2000; accepted 5 September 2000)

Short wavelength x-ray radiation microscopy is well suited for a number of material and life science studies. The x-ray microscope (XM1) at the Advanced Light Source Synchrotron in Berkeley, California uses two diffractive Fresnel zone plate lenses. The first is a large condenser lens, which collects soft x-ray radiation from a bending magnet, focuses it, and serves as a linear monochromator. The second is the objective zone plate lens, which magnifies the image of the specimen onto a high-efficiency charge coupled device detector. The objective lens determines the numerical aperture and ultimate resolution. New objective lens zone plates with a minimum linewidth of 25 nm and excellent linewidth control have been fabricated using Berkeley Lab's 100 keV Nanowriter electron beam lithography tool, a calixarene high-resolution negative resist, and gold electroplating. Although the condenser zone plate is less critical to the resolution of the instrument, its efficiency determines the flux on the sample and ultimately the exposure time. A new condenser zone plate was fabricated and has a 9 mm diameter, 44 000 zones, and a minimum zone width of 54 nm (optimally the condenser and objective should have the same zone width). It is also fabricated with the Nanowriter at 100 keV using poly(methylmethacrylate) resist and nickel electroplating. The phase shift through the nickel absorber material enhances the diffraction efficiency over an amplitude only zone plate. To evaluate the microscope's performance transmission test patterns have been made and imaged. Lineout data show modulation for 30 nm lines and 60 (1:2) spaces to be almost 100%. These new diffractive optical elements represent a significant advancement in the field of high-resolution soft x-ray microscopy. Diffractive optical elements have been used to measure the wave front error of an extreme ultraviolet projection optical system. The reference wave is generated by the spherical wave generated by diffraction from a small freestanding pinhole. © 2000 American Vacuum Society. [S0734-211X(00)11106-0]

## I. INTRODUCTION

In the soft x-ray region of the electromagnetic spectrum, materials suitable for fabricating refractive lenses are not available. Reflective focusing optics can be constructed using multilayer structures of different materials in limited wavelength regions as, for example, is used in extreme ultraviolet (EUV) lithography.<sup>1</sup> Large angle (grazing) incidence reflection can also be used to make focusing x-ray optics.<sup>2</sup> Optical elements based on diffraction, such as Fresnel zone plates, have shown very high resolution and are used in x-ray microscopes for probe formation and imaging. Instruments in which the x-ray beam is focused to a small spot and the sample or beam is scanned can provide a wealth of signals suitable for detection, transmitted x-ray intensity,<sup>3</sup> photoelectron<sup>4</sup> intensity and spectra, and fluorescence imaging.<sup>5</sup> In addition to probe formation, zone plates are used as imaging elements to magnify the radiation transmitted through an object onto a suitable detector in a conventional microscope configuration. The XM1 microscope at Berkeley Laboratory's Advanced Light Source Synchrotron is configured as a conventional x-ray microscope.<sup>6</sup>

The position of the zones for a Fresnel zone plate are given by the equation

$$R^2(m) = m\lambda f + (m\lambda)^2/4,$$

where  $R$  is the radius of the zone,  $m$  an integer is the zone number,  $\lambda$  is the wavelength, and  $f$  is the focal length. Provided that the zone plate has enough zones (about 100) the outer zones act like a localized grating with period  $2\delta$ , where  $\delta$  is the finest zone width. The numerical aperture of a zone plate is then  $\lambda/(2\delta)$  and this sets the scale for the resolution of the lens. Therefore, the requirement for high spatial resolution forces the fabrication of the smallest zone width possible. High-resolution electron beam lithography is well suited for exposing the fine feature zones and other diffractive optics structures with the necessary pattern placement accuracy.

## II. NANOWRITER HIGH RESOLUTION ELECTRON BEAM LITHOGRAPHY SYSTEM

Figure 1 shows a photograph of the lithography tool used for the fabrication of x-ray zone plates and other diffractive optical elements. This tool has the same electron optical column, stage, and support electronics of the Leica Microsystems VB6-HR<sup>7</sup> system coupled with a unique digital pattern generator (DPG), ideally suited for curved structures, and control software developed internally at Berkeley Laboratory.<sup>8</sup> The Leica column consists of a thermal field emission source for high brightness giving small probe size

<sup>a)</sup>Electronic mail: EHAnderson@lbl.gov

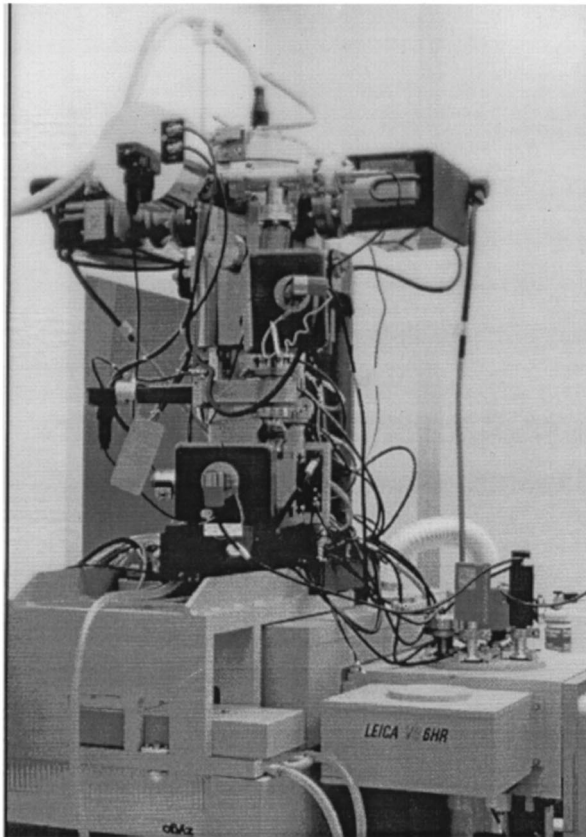


FIG. 1. Nanowriter electron beam lithography tool for ultrahigh resolution research and development lithography. Column, stage, and ancillaries built by Leica Microsystems. Digital Pattern Generator, data path, and control software developed at Lawrence Berkeley National Laboratory.

and high current. The accelerating voltage is variable between 20 and 100 kV with the best lithography results obtained at 100 kV. The stage has travel over approximately 150 mm by 150 mm area and incorporates a three axis ( $x$ ,  $y$ ,  $\theta$ ),  $\lambda/1024$  (0.6 nm) resolution interferometer for positional measurement, feedback, and control. The vacuum system uses oil-free dry turbo and backing pumps for clean contamination-free operation. The sample holders are initially pumped in a load-lock and are transported by a robotic arm either directly to the stage or to one of two holding areas for temperature conditioning. Holders made by Leica are front surface referenced for height control and allow 3, 4, 5, 6, and 8 in. wafers as well as 6 in. square by 1/4 and 1/8 in. thick mask plates to be used. A transmitted electron detector is mounted directly under the stage for on-axis alignment and calibration.

The DPG delivers  $X$  and  $Y$  analog deflection signals for both the major (slow-speed and large deflection) and minor (high-speed and small deflection) amplifiers. The minor field size is 1/64 of the major field size and the amplifier has a 25 MHz bandwidth. The fine focus,  $X$  and  $Y$  stigmation signals are dynamically corrected by the DPG and fed into the respective correction coil amplifiers. The blanking signal from the DPG drives the high-speed blanking plate amplifier using differential ECL signals. The critical DPG electronics is

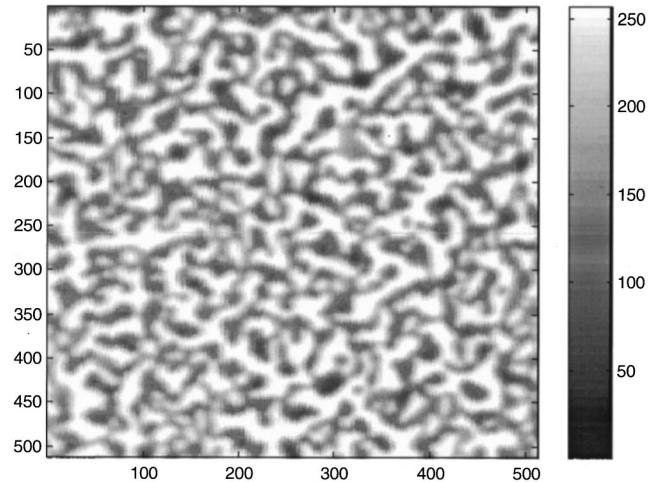


FIG. 2. Transmitted electron signal measured by the diode detector under the sample stage of gold "islands" used for alignment and calibration. The gold islands are formed by annealing 10 nm of evaporated gold for 60 min in a 170 °C oven on a 100 nm thick window of  $\text{Si}_3\text{N}_4$ . These structures have high-spatial resolution and a sharp autocorrelation function. The  $x$  and  $y$  units are 2 nm/pixels.

physically located near the column to minimize signal path lengths and degradation. The control computer "talks" to the Leica subsystems such as the electron optics, stage, and robot control using a 10 Mbit/s ethernet interface. The control computer has a frame grabber board and high-speed image coprocessor board to rapidly evaluate numerically intensive fast Fourier transform calculations for correlation based mark detection.

A window wafer made of a 100 nm  $\text{Si}_3\text{N}_4$  membrane with gold "islands" (10 nm evaporated gold annealed in air 60 min at 170 °C), is shown in Fig. 2, and is used to establish proper on-axis alignment. Using an automatic focus/stigmation algorithm that minimizes the size and nonroundness of the autocorrelation function, an array (typically 6 by 6) of data points is measured within the exposure field. The coefficients of a two dimensional polynomial function are determined by a singular value decomposition<sup>9</sup> of the measured data values. The corrections are applied and repeated if necessary. In the larger fields, nonlinear distortion corrections become important. The laser feedback control of the stage is next calibrated by first taking an image of a reference mark and then moving the stage a short distance within the feedback range. A new image is taken and the process is repeated for four different positions of the stage. Cross-correlation functions are used to determine the positional change between the initial mark position and four subsequent measured positions. Again singular value decomposition is used to determine the proper feedback linear terms from the overdetermined set of data. When the laser feedback is properly calibrated the reference mark will appear to be stationary with the stage moving to different positions. After laser feedback calibration, the nonlinear distortions of the exposure field are measured and corrected in a similar way. First, an image of a reference mark is recorded in the center of the field. The stage and deflection are moved together in a two-

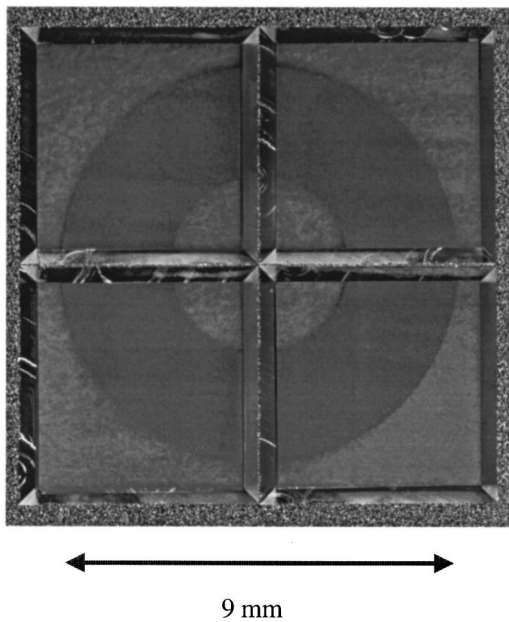


FIG. 3. Optical micrograph of the condenser zone plated fabricated using 100 keV electron beam lithography, PMMA resist, and nickel electroplating. The zone plate is 9 mm in diameter, has 41,000 zones, and a smallest zone width of 54 nm.

dimensional array throughout the field and subsequent images of the mark are taken at each point. The displacement at each point is determined by cross-correlation calculation between the reference image and mark image. Figure 3 shows the magnitude of the nonlinear corrections for a  $524 \mu\text{m}$  exposure field and the final correction values. Accurate beam placement is critical for diffractive optics since placement errors introduce phase errors and the phase relationships across the entire optic surface must be a small fraction of the smallest linewidth. For diffraction limited resolution the phase error should be smaller than  $\pi/8$  with a 25 nm outer zone width, the placement should be  $25 \text{ nm}/8 \text{ rms}$ , giving  $3\sigma$  placement of 9 nm or better. Finally, the minor field deflection is calibrated against the major field. A reference image is taken of a mark and compared with a set of four images taken with the minor field set to boundary limits and the major field set to an equal and opposite deflection. When properly aligned the reference mark remains stationary and deviations from the reference location are analyzed to apply corrections to the minor field scaling and rotation terms.

### III. ZONEPLATE FABRICATION PROCESSING

A number of resist processes are used to take advantage of sensitivity and resolution tradeoffs. The resist with the highest resolution, “4-methyl-1-acetoxycalix[6]arene”<sup>10,11</sup> also has the highest dose requirement. For the condenser zone plate, 950 molecular weight poly(methylmethacrylate) (PMMA) resist<sup>12</sup> was used. For other applications resists based on DUV chemically amplified products are used.<sup>13–15</sup> The membrane windows for both the condenser and objective zone plates are formed by back etching a 100 nm thick  $\text{Si}_3\text{N}_4$  coated wafer. The condenser window consists of four

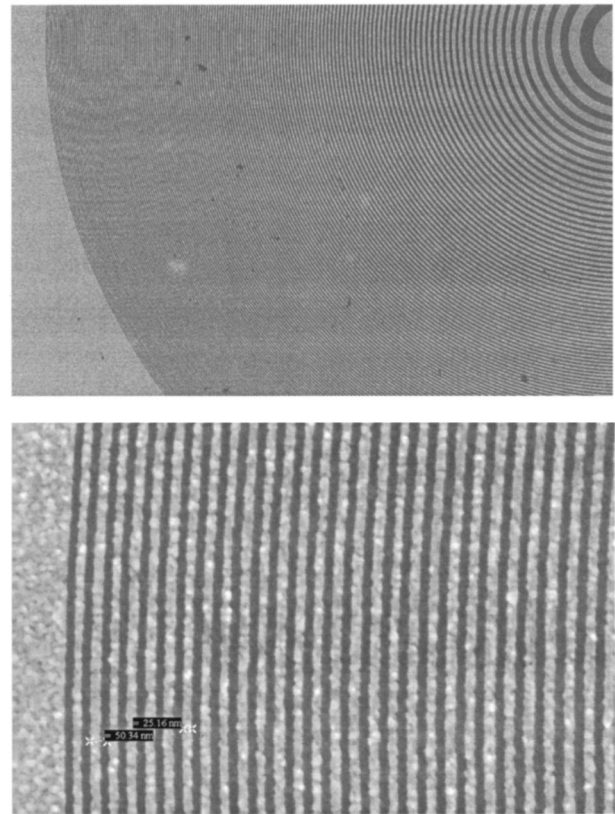


FIG. 4. SEM of an objective, microzoneplate. The outer zones, shown at the bottom are 25 nm and good linewidth control is observed across the structure.

5 mm square sections with “support” silicon structures. Larger windows, 10 mm by 10 mm, were first used but found to be easily broken during processing, and the area lost to the support structure was a small compromise necessary to achieve acceptable yield. Figure 4 shows the condenser zone plate and the support structure. A thin electroplating base of 5 nm chrome and 12 nm gold is evaporated onto the window wafer. A coating of PMMA is spun onto the wafer and baked at  $170^\circ\text{C}$  for 90 min to form a thickness of 250 nm. The wafer is exposed with a 100 kV electron beam at a current of about 2.3 nA, slightly compromising ultimate system resolution but necessary to finish the exposure in a reasonable time, approximately 48 h. The wafer is developed in 2:1 ratio of isopropyl alcohol (IPA) and methyl-iso-butyl-ketone for 45 s, rinsed in IPA, and carefully dried with  $\text{N}_2$ . The zone plate is then given a short plasma clean in oxygen to remove contamination from the plating base, typically removing 10 nm of PMMA. The wafer is electroplated in a commercial nickel plating solution<sup>16</sup> with an apparatus developed to keep the solution clean and at a constant temperature. The plating progress is monitored by measurement of the difference in step height between the plated areas and the PMMA resist in an off zone plate test structure. After the plating is completed the PMMA is stripped in solvents and the wafer is cleaned.

The processing for the objective zone plate starts with a thin  $100 \mu\text{m}$  thick window wafer (due to the mechanical requirements of the XM1 microscope) with 100 nm  $\text{Si}_3\text{N}_4$

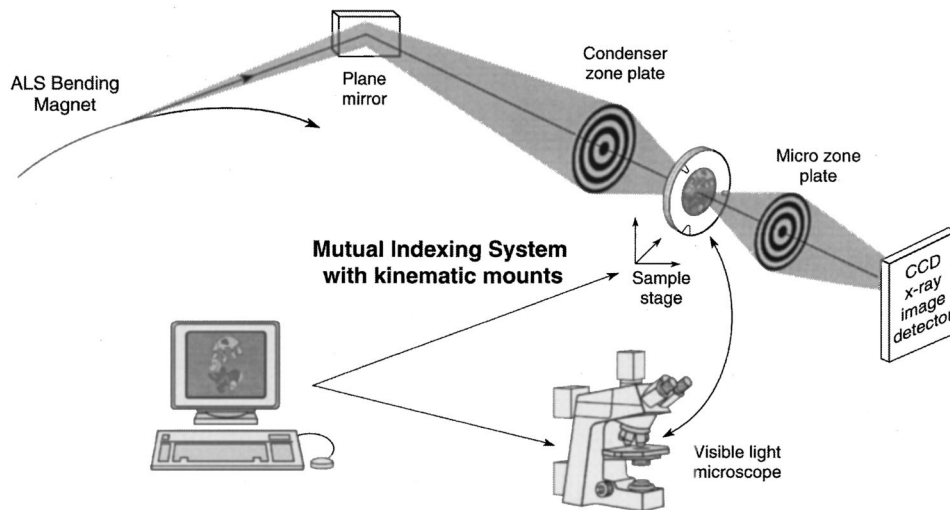


FIG. 5. Layout of XM1 x-ray microscope at the Advanced Light Source Synchrotron. The broad band radiation from a bending magnet is reflected off a nickel mirror at grazing incidence onto the condenser zone plate. This zone plate focuses the beam onto the sample. The condenser zone plate and the aperture at the sample plane form a linear monochromator. The radiation transmitted through the sample is imaged with high magnification onto the back thinned CCD detector.

membrane. Previous work demonstrated that calixarene resist produced smaller linewidth zone plates than PMMA.<sup>10</sup> The full chemical name of this resist is “4-methyl-1-acetoxycalix[6]arene” and was purchased from the chemical company TCI America.<sup>17</sup> This material did not fully dissolve in the solvent *o*-dichlorobenzene but fortunately when a small amount of dichloromethane was added the material dissolved. The calixarene resist is spin coated after chrome-gold plating base is evaporated and baked in an oven at 170 °C for 30 min. The wafer is exposed under high-resolution beam conditions at 100 kV, 0.5 nA beam current at a dose of about 27 000  $\mu\text{C}/\text{cm}^2$ . These very high dose and high-resolution beam conditions result in relatively long exposures (10 min each zone plate). The basic stability of the tool is required to complete the exposure without significant drift or change during the exposure time. The exposed samples are developed in xylenes for 30 s and rinsed in IPA for 30 s. The wafer is oxygen cleaned and plated in a commercial gold solution.<sup>18</sup> A scanning electron-microscope (SEM) micrograph showing the electroplated structure is shown in Fig. 4. The gold lines at the edge of the zone plate have a linewidth of 25 nm and good linewidth control is observed across the sample. This is necessary but not sufficient for diffraction limited operation since zone placement is critical. The condenser and objective zone plates are installed at the XM1 microscope and used to study a variety of scientific samples.

#### IV. X-RAY MICROSCOPY IMAGES FROM XM1

The layout of the XM1 microscope beam line is shown in Fig. 5. The radiation from the bending magnet is reflected off a nickel coated flat mirror to remove the higher energy x rays, and collected by the condenser zone plate. The condenser focuses the radiation onto the sample through a small aperture, the combination of which forms a linear monochromator. Wavelengths longer or shorter than the desired wavelength are focused behind and ahead of the aperture, respectively. The soft x rays transmitted through the sample are imaged by the objective zone plate onto a sensitive back-

thinned charge coupled device (CCD) detector equipped with low noise readout electronics. Figure 6 shows a x-ray micrograph of thin gold 30 nm wide lines and 60 nm space grating and corresponding intensity lineout. The modulation of the lineout is almost 100%. Figure 7 shows 18 nm lines and 54 nm spaces with a high modulation lineout. Research is ongoing to determine the ultimate resolution limit of the system, which is estimated to be in the 20 nm range.

#### V. DIFFRACTIVE OPTICS FOR PHASE SHIFTING POINT DIFFRACTION INTERFEROMETRY

The development of optical systems for EUV lithography requires an accurate measurement of the system’s wave front. A phase shifting point diffraction interferometer (PDI) described by Goldberg *et al.*<sup>19</sup> is used for these measurements. The wave front under test is passed unperturbed through an aperture and a spherical wave front is produced by a small pinhole. The interference between these two patterns is recorded on a CCD detector and analyzed by a computer to determine the wave front aberrations. The critical diffractive element is this mask which contains the aperture

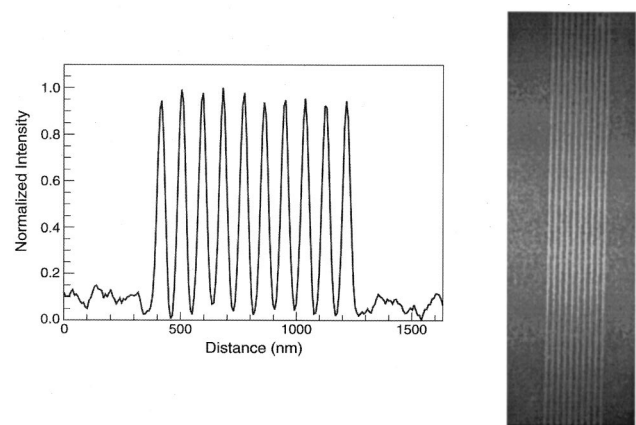


FIG. 6. X-ray micrograph of thin gold 30 nm lines and 90 nm period grating and corresponding intensity lineout. The modulation is almost 100%.

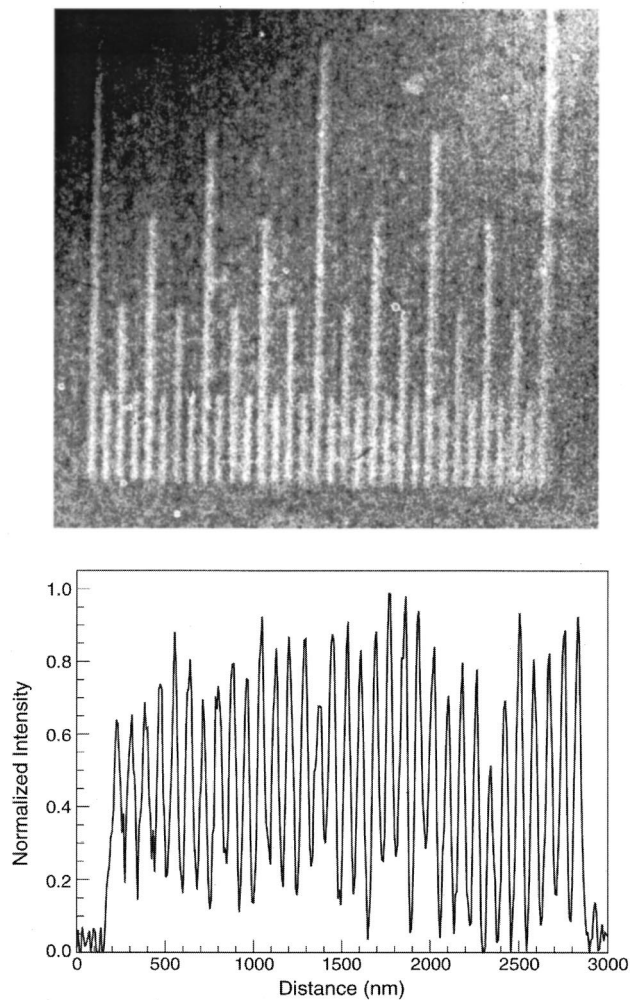


FIG. 7. X-ray micrograph of thin 18 nm lines and 72 nm period grating.

and pinhole, both of which must be “freestanding” to eliminate the introduction of artifacts from phase shifts in the membrane and the potential of beam induced contamination buildup. Figure 8 shows the PDI mask structure prior to etching. A wafer with  $\text{Si}_3\text{N}_4$  windows is spin coated with a positive chemically amplified resist (KRS) invented by IBM.<sup>13</sup> The wafers are soft baked on a hot plate for 2 min at 110 °C and the aperture and pinhole patterns are exposed with 100 kV lithography and developed using diluted MF312 developer. A postexposure bake is not required. The pattern is transferred by reactive ion etching of the  $\text{Si}_3\text{N}_4$  all the way through the membrane. Care must be exercised to avoid overetching which will cause window breaking. After etching the absorber material, nickel is evaporated on both the front side and back side of the wafer. About 240 nm of nickel (total) can be evaporated before the added stress breaks the windows.

## VI. CONCLUSION

Diffractive optical elements for x-ray applications stress the limits of nanofabrication due to the demanding requirements for fine linewidth structures and accurate image place-

80 - 120 nm Pinholes

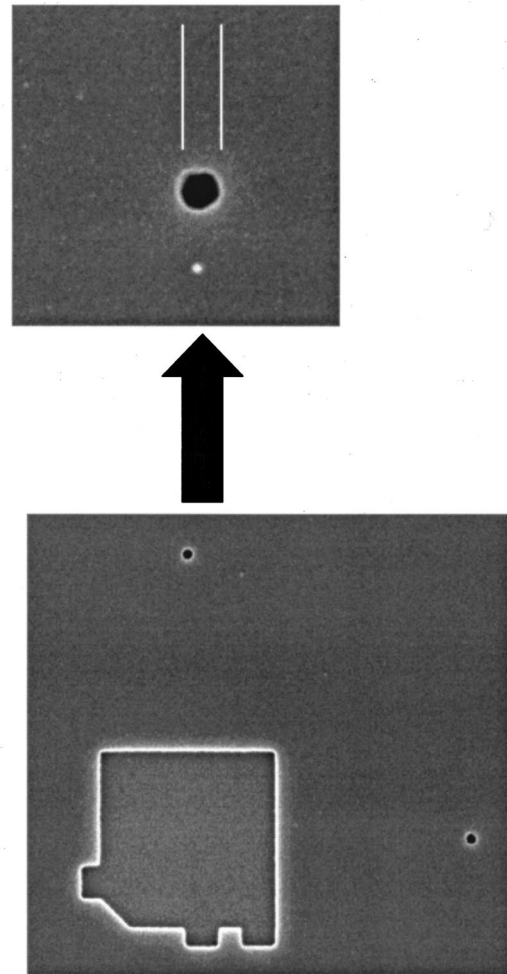


FIG. 8. SEM micrograph of phase shift point diffraction interferometer object structure used to pass the primary beam unaltered and generate a spherical reference beam. The interference pattern between the primary beam and the reference beam is recorded on a CCD imager and processed to provide information about the primary beam wave front.

ment. A high-resolution electron beam lithography tool, which incorporates unique pattern generation hardware, has been used to fabricate large condenser zone plates and 25 nm outer zone width objective zone plates. These Fresnel lenses have been installed at the XM1 x-ray microscope and used for a number of projects in life science and material science research. A free standing diffractive structure for a common-path phase shifting point diffraction interferometer was fabricated and used to make high-accuracy measurements of a large four mirror EUV optical system. The electron beam lithography tool has proven its capability to pattern fine linewidth structures with excellent pattern placement.

## ACKNOWLEDGMENTS

This work was supported by the Defense Advanced Research Project Agency Advanced Lithography Program through the U.S. Department of Energy under Contract No. DE-AC03-76SF00098. The authors gratefully acknowledge

the contributions of Volker Boegli and Lawrence Muray in the electron beam lithography tool development, the late Werner Meyer-Ilse for x-ray microscopy with zone plate optics, Ken Goldberg and Patrick Naulleau for PID mask development, and Linda Geniesse for artwork preparation.

<sup>1</sup>D. Tichenor *et al.*, Proc. SPIE **3997**, 48 (2000).

<sup>2</sup>P. Kirkpatrick and A. V. Baez, J. Opt. Soc. Am. **38**, 766 (1948).

<sup>3</sup>C. Jacobsen, S. Williams, E. Anderson, M. T. Browne, C. J. Buckley, D. Kern, J. Kirz, M. Rivers, and X. Zhang, Opt. Commun. **86**, 351 (1992).

<sup>4</sup>H. Ade, Ph.D. thesis, Physics Department, SUNY, Stony Brook, 1990.

<sup>5</sup>C. Jacobsen, S. Lindaas, S. Williams, and X. Zhang, J. Microsc. **172**, 121 (1993).

<sup>6</sup>W. Meyer-Ilse, T. Warwick, and D. Attwood, *X-Ray Microscopy* (AIP, New York, 1999), p. 129.

<sup>7</sup>B. H. Koek, T. Chisholm, A. J. V. Run, J. Romijn, and J. P. Davey, Microelectron. Eng. **23**, 81 (1994).

<sup>8</sup>E. H. Anderson, V. Boegli, and L. P. Muray, J. Vac. Sci. Technol. B **13**, 2529 (1995).

<sup>9</sup>W. H. Press, B. P. Flannery, S. A. Teukolsky, and W. T. Vetterling,

*Numerical Recipes* (Cambridge University Press, Cambridge, UK, 1986), p. 52.

<sup>10</sup>J. Fujita, Y. Ohnishi, Y. Ochiai, and S. Matsui, Appl. Phys. Lett. **68**, 1297 (1996).

<sup>11</sup>S. Spector, C. Jacobsen, and D. Tennant, J. Vac. Sci. Technol. B **15**, 2872 (1997).

<sup>12</sup>Microlithography Chemical Company, 294 Pleasant St., Watertown, MA 02172.

<sup>13</sup>K. Y. Lee and W. S. Huang, J. Vac. Sci. Technol. B **11**, 2807 (1993).

<sup>14</sup>Z. Cui, A. Gerardino, M. Gentili, E. DiFabrizio, and P. D. Prewett, J. Vac. Sci. Technol. B **16**, 3284 (1998).

<sup>15</sup>E. A. Dobisz and C. R. K. Marrian, J. Vac. Sci. Technol. B **15**, 2327 (1997).

<sup>16</sup>Sulfamex make up solution, Enthone Omi, 350 Frontage Rd., West Haven, CT 06516.

<sup>17</sup>TCI America, 9211 North Harborsgate St., Portland, OR 97203.

<sup>18</sup>BDT510 make up solution, Enthone Omi, 350 Frontage Rd., West Haven, CT 06516.

<sup>19</sup>K. A. Goldberg, P. Naulleau, P. Batson, P. Denham, E. H. Anderson, H. Chapman, and J. Bokor, J. Vac. Sci. Technol. B, these proceedings.